Physica B 406 (2011) 541–544

Contents lists available at ScienceDirect

Physica B

journal homepage: www.elsevier.com/locate/physb

Effect of size on dielectric constant for low dimension materials

M. Tian [a], M. Li [b,*], J.C. Li [a,*]

[a] Key Laboratory of Automobile Materials (Jilin University), Ministry of Education and School of Materials Science and Engineering, Jilin University, Changchun 130022, China
[b] Department of Physics, Huaibei Normal University, Huaibei 235000, China

ARTICLE INFO

Article history:
Received 14 September 2010
Received in revised form
10 November 2010
Accepted 10 November 2010

Keywords:
Dielectric constant
Dimension materials
Size-dependence

ABSTRACT

Based on the consideration on size-dependent root of mean-square displacement of vibration of atoms (rms) $\sigma(D)$, where D denotes the diameter of nanoparticles and nanowires or the thickness of thin films, size-dependent dielectric constants of low-dimensional materials are modeled without any adjustable parameter. The model predicts a decrease or an increase in dielectric constants with drop of D. The predicted results correspond to experimental and other theoretical results for particles and thin films of Si, CdSe, GaAs, H_2O and thiol.

1. Introduction

As size of materials decreases to nanometer size range, many properties of the materials change dramatically, which has led to new technological applications of media with tunable properties and will find immense potential applications in the area of optoelectronic devices [1–4]. One of such material properties is the dielectric constant ε. The modification of ε affects the Coulomb interaction among electrons, which leads to the variation in the activation (electron–hole pair) energies and thus would significantly change the optical absorption and transport properties of semiconductor devices [5]. Thus, the size dependence of ε has attracted considerable interest both experimentally and theoretically.

It was found that ε value is a function of D [5–20], where D shows the diameter of particles and wires or the thickness of films, such as Si [5–10], CdSe [11–13], GaAs [19], H_2O [20] and thiol [21]. Some early experimental results show that the ε values of nanosized materials are lower than that of the bulk, or $\varepsilon(D)<\varepsilon(\infty)$, where ∞ denotes the bulk size [5,11,14,16,17], which are confirmed by first-principles calculations and other theoretical methods [7,8,10,12,18]. However, a recent experiment shows that ε values of thin films can have an opposite trend when there is hydrogen bonding on the film/substrate [21].

Meanwhile, the $\varepsilon(D)$ function of Si has theoretically been modeled with good correspondence of experiments [5,6,22,23]. However, all models have not predicted increase in $\varepsilon(D)$ function as D decreases. In addition, some models are phenomenological one with adjustable parameters being lack of physical meanings [23], and some models are complicated and cannot be easily utilized [6,22]. The interfacial effect and shape effect on $\varepsilon(D)$ function need also to be quantitatively considered.

In this contribution, a simple thermodynamic model, free of any adjustable parameter, is developed. The model has predicted the depression of $\varepsilon(D)$ functions of nanocrystals with size. The especial emphasis is made on the interface effect and shape effect on $\varepsilon(D)$ functions. Agreement among our work and other experimental and theoretical results are found.

2. Model

It has been reported that the relative change of the dielectric susceptibility, $\chi=\varepsilon-1$, can be modeled as [5]

$$\frac{\Delta\chi(D)}{\chi(\infty)}=-2\frac{\Delta E_g(D)}{E_g(\infty)} \tag{1}$$

where E_g and Δ denote band-gap and the change respectively.

As is known that $\Delta E_g(D)=2[Q(\infty)-Q(D)]$ and $E_g(\infty)=2Q(\infty)$ [24], where $Q(D)$ and $Q(\infty)$ are the size-dependent activation energy for the electrical migration of nanocrystals and bulk materials, respectively.

According to the Arrhenius relationship of $\rho(\infty,T)=\rho_0(\infty)\exp[-Q(\infty)/k_BT]$, where $\rho(\infty,T)$ and ρ_0 are the temperature-dependent electrical resistivity of bulk crystals and a pre-exponent constant, respectively, k_B is Boltzmann's constant. If this relationship may be generalized for the corresponding size and temperature dependences of electrical resistivity $\rho(D,T)$

$$\rho(D,T)=\rho_0(D)\exp[-Q(D)/k_BT]. \tag{2}$$

To establish $Q(D)$ function, the ρ value at melting temperature T_m is understandably assumed to be size independent, or

* Corresponding authors. Tel.: +86 431 85095371; fax: +86 431 85095876.
E-mail addresses: li_ming2009@yahoo.cn (M. Li), ljc@jlu.edu.cn (J.C. Li).

0921-4526/$ - see front matter © 2010 Elsevier B.V. All rights reserved.
doi:10.1016/j.physb.2010.11.034

$\rho[D,T_m(D)]=\rho[\infty,T_m(\infty)]$. Thus, $\rho[D,T_m(D)]=\rho_0(D)\exp\{-Q(D)/[k_BT_m(D)]\}=\rho_0(\infty)\exp\{-Q(\infty)/[k_BT_m(\infty)]\}$. Since the exponential coefficient $Q(D)$ plays an essential role on the size of $\rho(D,T)$ function, $\rho_0(D)\approx\rho_0(\infty)$ is assumed as a first-order approximation. As a result, it reads

$$Q(D)/Q(\infty)=T_m(D)/T_m(\infty). \quad (3)$$

It is known that the size-dependent $T_m(D)$ function has the following form [25]:

$$\frac{T_m(D)}{T_m(\infty)}=\exp\left(-\frac{(\alpha-1)}{(D/D_0-1)}\right) \quad (4)$$

where α is a function of surrounding conditions of low-dimensional crystals, which has the following expression [25]:

$$\alpha=\sigma_s^2(D)/\sigma_v^2(D) \quad (5)$$

where $\sigma_s(D)$ and $\sigma_v(D)$ are the mean-square displacements of vibration of atoms (rms) of surface and interior atoms, respectively. D has a usual meaning of diameter for particles or wires. For a film, D denotes its thickness. D_0 denotes a critical diameter at which almost all atoms of a low-dimensional material are located on its surface. We define $2D_0$ as the smallest size of low-dimensional materials in crystalline form where a half of atoms are located on the surface or interface of the nanomaterials [25]. Thus, $2D_0$ is the lowest size limit what our model can be utilized to determine $\varepsilon(D)$ functions. As results, in the following figures, the predicted sizes are limited between $2D_0$ and bulk where the nanocrystals remain their bulk structures, which is also the premise of the above utilized equations [25]. Note that D_0 depends on dimension d and atomic diameter h through [26,27]

$$D_0=2c(3-d)h. \quad (6)$$

In Eq. (6), $d=0$ for particles, $d=1$ for rods or wires and $d=2$ for films. When a nanoparticle is deposited on an inert substrate, it may wet or not wet the substrate. When the deposit does not wet the substrate, the deposit will preferably take a spherical shape, which has the smallest surface/volume ratio where its dimension $d=0$. If the deposit wets the substrate, the particle shape may be island-like or disk-like, $d=1$ as its quasi-dimension is assumed [28]. The constant c shows the normalized surface (interface) area where the atomic potential differs from that of the interior of the low-dimensional crystal [27].

For organic molecular crystals, since the shape of an organic molecule is usually not spherical, h is defined as its mean size of a segment of chain molecules [29]

$$h=[V_m/(nN_0)]^{1/3} \quad (7)$$

where V_m is the molar volume, n denotes the segment number of the chain and N_0 the Avogadro constant.

Since $\varepsilon=\chi+1$, in light of Eqs. (1)–(4), we have

$$\frac{\varepsilon(D)-\varepsilon(\infty)}{\varepsilon(\infty)-1}=2\left\{\exp\left(-\frac{(\alpha-1)}{(D/D_0-1)}\right)-1\right\}. \quad (8)$$

In Eq. (8), α values of nanocrystals in different surface or interface states are different. For free-standing low-dimensional crystals or those supported by a passivated substrate where there is a weak chemical interaction between the crystal and the substrate by Van der Waals forces, the corresponding α or α_s can be determined by [26]

$$\alpha_s=[2S_{vib}(\infty)/(3R)]+1 \quad (9)$$

where $S_{vib}(\infty)$ is the bulk vibrational melting entropy and R the ideal gas constant. For semiconductors, electronic state changes from semiconductors to metals leads to a large contribution on bulk overall melting entropy $S_m(\infty)$ [30]. If the corresponding $S_{vib}(\infty)$ is unavailable, a rough estimation on $S_{vib}(\infty)$ is estimated as [30]

$$S_{vib}(\infty)\approx S_m(\infty)-R. \quad (10-1)$$

However, for metallic and organic crystals, $S_m(\infty)$ is essentially contributed by its vibrational part [31], or

$$S_{vib}(\infty)\approx S_m(\infty). \quad (10-2)$$

When the nanocrystals are supported by a substrate, one side of the nanocrystals is a nanocrystal/substrate interface. If there is a much weak chemical interaction on the interface in comparison with that within the crystals, this interface is approximately considered as surface. In this case, Eq. (9) is still utilizable. When the chemical interaction on the nanocrystal/substrate interface is strong enough in comparison with that within the nanocrystals, this interface cannot be viewed as an equivalent surface. α value on this interface α_i must be specially considered. With a similar definition, $\alpha_i=\sigma_i^2(D)/\sigma_v^2(D)$, where the subscript i denotes the interface. Since $\alpha_s=\sigma_s^2(D)/\sigma_v^2(D)$, $\alpha_i=\alpha_s\sigma_i^2(D)/\sigma_s^2(D)$. It is assumed $\sigma_s^2(D)\propto 1/E_s$ and $\sigma_i^2(D)\propto 1/E_i$, where E denotes the bond strength. Thus

$$\alpha_i=\alpha_sE_s/E_i. \quad (11)$$

Assuming that the effects of both surface and interface of nanocrystals on $\varepsilon(D)$ values is additive, it gives

$$\frac{\varepsilon(D)-\varepsilon(\infty)}{\varepsilon(\infty)-1}=\left\{\left\{\exp\left(-\frac{(\alpha_i-1)}{(D/D_0-1)}\right)-1\right\}+\left\{\exp\left(-\frac{(\alpha_s-1)}{(D/D_0-1)}\right)-1\right\}\right\}/2. \quad (12)$$

3. Results and discussion

Comparisons between the model predictions in term of Eq. (8) and the experimental and other theoretical results for $\varepsilon(D)$ values of Si nanoparticles and films on inert substrates are shown in Fig. 1. $\varepsilon(D)$ function decreases as D decreases. As the chemical interaction of Van der Waals forces on the interface is negligible in comparison with the internal potential within the nanocrystals, $c=1$ can be used. The model prediction corresponds to the theoretical and the experimental evidences.

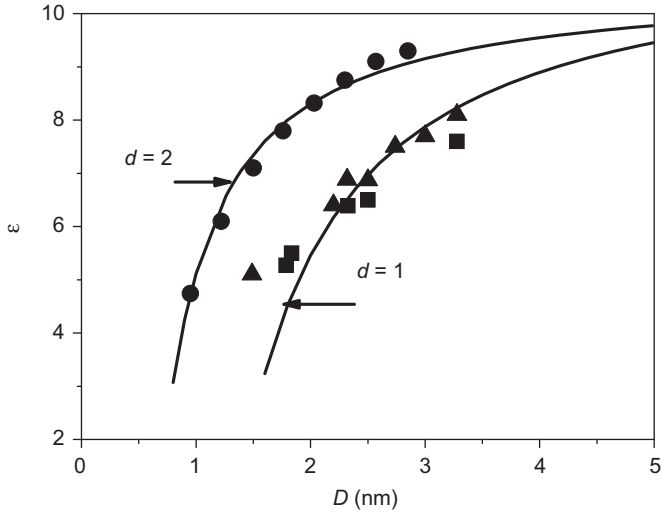

Fig. 1. $\varepsilon(D)$ functions of Si particles and thin films. The solid lines denote the model predictions in terms of Eqs. (8) and (9). For particles shown in (a), $D_0=4h=0.768$ nm in terms of Eq. (6) with $d=1$ and $c=1$ for free-standing interface and other related parameters are listed in Table 1. $\varepsilon(\infty)=11.4$, which is a mean value [6] since there is no $\varepsilon(\infty)$ value in the references relating experimental data of $\varepsilon(D)$ [9]. The symbol ! and 7 [9], are corresponding theoretical results. For thin films shown in (b), $D_0=2h$ in terms of Eq. (6) with $d=2$ and $c=1$ is used. $\varepsilon(\infty)=10.62$ [10]. The symbols, [10] denote the corresponding experimental results.

Fig. 2 shows a comparison for $\varepsilon(D)$ function of CdSe particles between the model prediction in terms of Eqs. (8) and (9) and the experimental results [11]. Note that although the surface of the CdSe particles is capped with organic ligands [11], the chemical interaction of the Van der Waals forces between the particles and the ligands is similar to that within the nanoparticles and the particle/liquid interface can be considered as a surface and $c=1/2$ is taken. The model prediction is in agreement with the experimental results.

Fig. 3 shows a comparison for $\varepsilon(D)$ function for GaAs particles between the model predictions in terms of Eqs. (8) and (9) and the experimental result [19]. As the surface of the particles is passivated by hydrongen-like atoms with partial charges, which resembles real passivations, filling all surface dangling bonds, $c=1$ is used. It shows that $\varepsilon(D)$ function decreases with decrease in size and the model prediction result is in agreement with the experimental result.

Fig. 4 shows $\varepsilon(D)$ function of water nanoparticles in terms of Eq. (8) where the particles are confined in a nanosized spherical cavity. As the liquid water is confined in a spherical nanocavity and the effective radius is defined to be the radial distance of the cavity wall from the centre where the water–surface interaction becomes zero, $c=1$ is defined. As shown in the figure, $\varepsilon(D)$ function decreases as D decreases. The reduction of $\varepsilon(D)$ is purely a result of confinement. The model prediction corresponds to the experimental results.

Fig. 5 shows $\varepsilon(D)$ function of thiol films in terms of Eq. (12) where the films are between an Au substrate and liquids. $\varepsilon(D)$

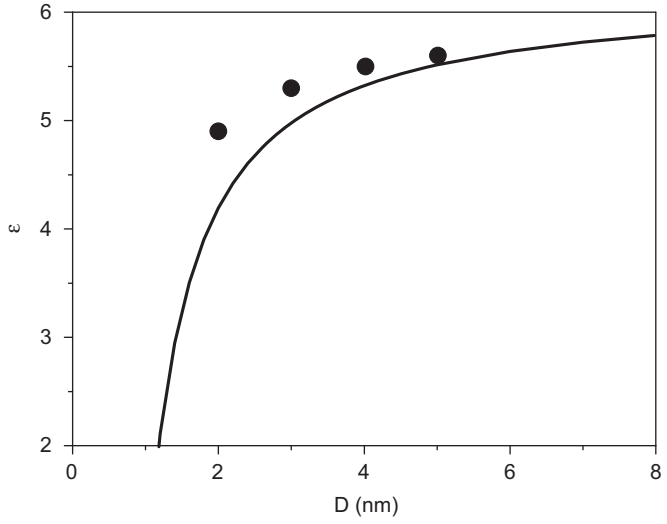

Fig. 2. $\varepsilon(D)$ function of CdSe particles. The solid line denotes the model prediction in terms of Eqs. (8) and (9) where $D_0=3h=0.447$ nm with $d=0$ and $c=1/2$ (due to the fact that the chemical interaction of the Van der Waals forces between the particles and the ligands is similar to that in the nanoparticles) in terms of Eq. (6). $\varepsilon(\infty)=6.2$ [12]. Other parameters are also listed in Table 1. The symbol , [11] denotes the corresponding experimental results.

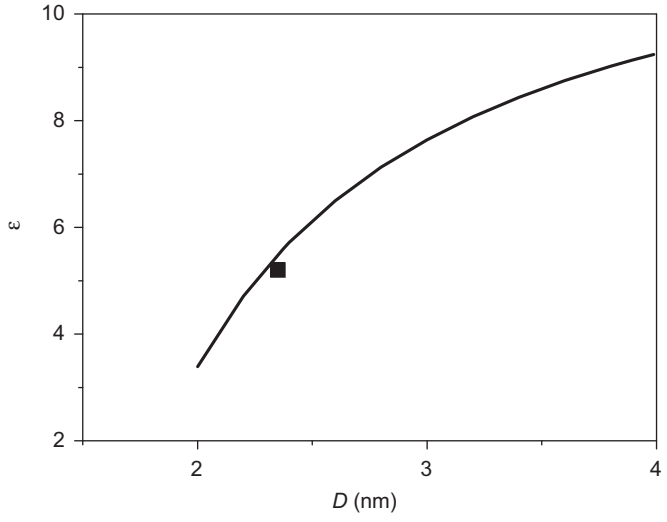

Fig. 3. $\varepsilon(D)$ function of GaAs particles. The solid line denotes the model prediction in terms of Eqs. (8) and (9) where $D_0=6h=1.06$ nm with $d=0$ and $c=1$ in terms of Eq. (6). $\varepsilon(\infty)=12.8$[19]. Other parameters are also listed in Table 1. The symbol ! [19] denotes the corresponding experimental results.

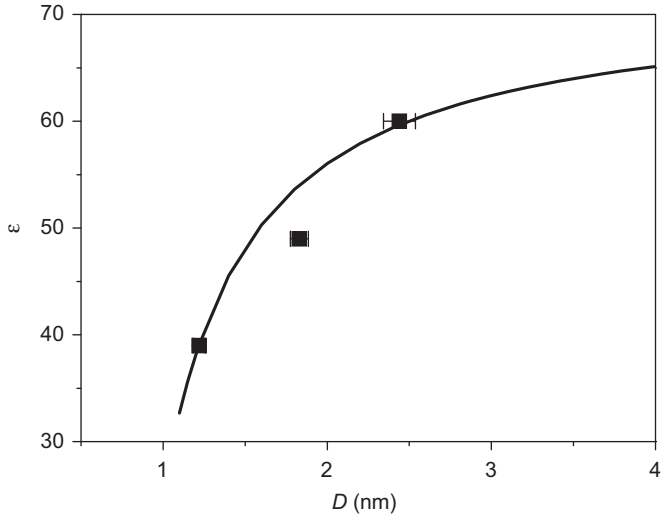

Fig. 4. . $\varepsilon(D)$ function of water nanoparticles in terms of Eq. (8) where the particles are confined in a nanodimensional spherical cavity. The solid lines denote the model prediction in terms of Eqs. (8) and (9) where $D_0=6h=0.577$ nm with $d=0$ and $c=1$ in terms of Eq. (6). $\varepsilon(\infty)=72$ [20]. Other parameters are also listed in Table 1. The symbol ! [20] denotes the corresponding experimental results.

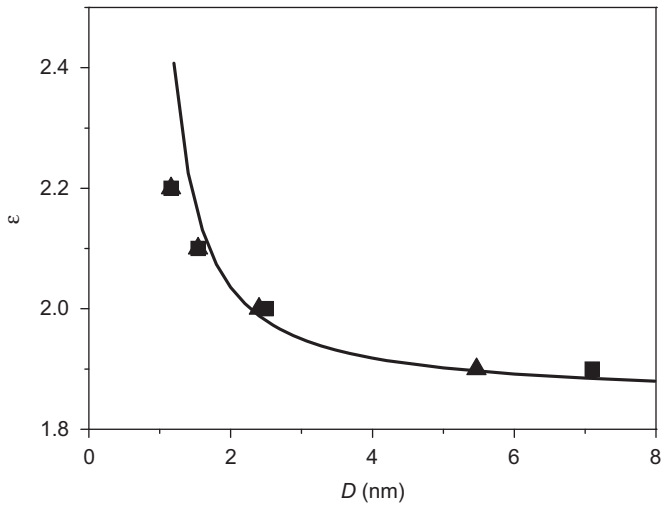

Fig. 5. $\varepsilon(D)$ function of thiol thin films that have hydrogen bonds on the interface. The solid line denotes the model prediction in terms of Eqs. (11) and (12) where $D_0=2h=0.598$ nm with $d=2$ and $c=1$ in terms of Eq. (6). $\varepsilon(\infty)=1.85$ [21]. $E_i=0.525$ J g-atom^{-1} is the mean value of hydrogen-bonding strength of thiol between 0.467and 0.583 J g-atom^{-1} [37], and $E_s=0.175$ J g-atom^{-1} shows the mean value of Van der Waals force between 0.117 and 0.233 J g-atom^{-1} [37]. $\alpha_i=0.395$ is obtained for film/liquid interface according to Eqs. (11) and (9) and Table 1. The symbols ! and 7 denote the experimental results where the film/liquid interfaces are ethanol, and binary ethanol/deionised water [21].

Table 1
Necessary parameters used in Eq. (12).

	h (nm)	$S_{vib}(\infty)$(J g-atom^{-1} K^{-1})
Si	0.192[a]	6.72 [35]
CdSe	0.219[b]	6.596[d]
GaAs	0.175[a]	23.186[d]
H_2O	0.096[a]	7.34 [29]
thiol	0.299[c]	2.31[e]

[a] In terms of $h=\{[3V/(4\pi)]^{1/3}\}/2$ with $V=a^3$ denoting the volume of one cell where $a=0.543$ nm and 0.565 for Si [32] and GaAs [33], respectively.

[b] In light of the same relation stated above, the crystal has a wurtzite structure with $a=0.43$ nm, $c=0.7011$ nm [12].

[c] In terms of Eq. (7), V_m is determined by M/ρ, with M being the molecular weight and ρ being the solid density cited from [34]. In light of the shortage of the data of 11-mercaptoundecanoic acid, the 3-thiadodecamoic acid is used instead, which has the same atom numbers with the same quantity, but different positions of S. $n=12$ for thiol.

[d] $S_{vib}(\infty)$ is determined by Eq. (10-1) with $S_m(\infty)=14.91$ J g-atom^{-1} K^{-1} [35] and 31.5 J g-atom^{-1} K^{-1}[35] for CdSe and GaAs, respectively.

[e] Due to short of $S_m(\infty)$ of thiol, $S_m(\infty)$ value of undecanoic acid is used and $S_{vib}(\infty)\approx S_m(\infty)=2.31$ J g-atom^{-1} K^{-1} [36] in terms of Eq. (10-2).

function increases as D decreases due to the strong interaction at the thiol/liquid interface where hydrogen bonding is present, which is stronger than that of Van der Waals forces within the thiol film where $c=1$ is taken. The model prediction is again in agreement with the experimental results.

Considering the mathematical relation of $\exp(-x)\approx 1-x$ when x is small enough as a first-order approximation, Eqs. (8) and (12) can be rewritten as

$$\frac{\varepsilon(D)-1}{\varepsilon(\infty)-1}\approx 1-\frac{D_0(\alpha-1)}{D}. \tag{13}$$

Hence, $(\varepsilon(D)-1)/(\varepsilon(\infty)-1)=1-C/D$ where $C=D_0(\alpha-1)$. The change in $\varepsilon(D)$ indicates that the most important size effect for low-dimensional materials is related with the surface/volume ratio, namely $1/D$. This is also consisted with other theoretical results. However, as the size of the nanocrystals further decreases to the size being comparable with the atomic or molecular diameter, namely about several nanometers, Eqs. (13) is no more suitable for predicating $\varepsilon(D)$ functions. Due to the surface lattice relaxation and the restrain from the lattice misfit between nanocrystals and substrates, the parameter α is introduced. When $\alpha>1$, $\varepsilon(D)$ will decrease with the decrease of D, while the contrary occurs when $0<\alpha<1$ (Table 1).

As shown earlier, $\varepsilon(D)$ function of different substances can be predicted as long as the surface (interface) conditions and related bulk thermodynamic parameters of the low-dimensional crystals are known.

4. Conclusion

In conclusion, $\varepsilon(D)$ function of nanocrystals in different shapes and interface conditions has been established based on a thermodynamic model. With different interface conditions and shape of nanocrystals, $\varepsilon(D)$ function can increase or decrease as D decreases. Consistency between the model predictions and the observations confirms the utility of the model.

Acknowledgements

The financial supports from National Key Basic Research and Development Program (Grant no. 2010CB631001) and Program for Changjiang Scholars and Innovative Research Team in University are acknowledged.

References

[1] L.T. Canham, Appl. Phys. Lett. 57 (1990) 1046.
[2] A.D. Yoffe, Adv. Phys 50 (2001) 1.
[3] C.Q. Sun, Prog. Mater. Sci. 48 (2003) 521.
[4] S. Sapra, D.D. Sarma, Phys. Rev. B 69 (2004) 125304.
[5] L.K. Pan, C.Q. Sun, T.P. Chen, S. Li, C.M. Li, B.K. Tay, Nanotechnology 15 (2004) 1802.
[6] R. Tsu, D. Babic, L. Loriatti Jr., J. Appl. Phys. 82 (1997) 1327.
[7] J.P. Walter, M.L. Cohen, Phys. Rev. B 2 (1970) 1821.
[8] L.W. Wang, A. Zunger, Phys. Rev. Lett. 73 (1994) 1039.
[9] M. Lannoo, C. Delerue, G. Allan, Phys. Rev. Lett. 74 (1995) 3415.
[10] C. Delerue, M. Lannoo, G. Allan, Phys. Rev. B. 68 (2003) 115411.
[11] C.B. Murray, D.J. Norris, M.G. Bawendi, J. Am. Chem. Soc. 115 (1993) 8706.
[12] L.W. Wang, A. Zunger, Phys. Rev. B 53 (1996) 9579.
[13] C.Q. Sun, X.W. Sun, B.K. Tay, S.P. Lau, H.T. Huang, S. Li, J. Phys. D: Appl. Phys. 34 (2001) 2359.
[14] B.T. Lee, C.S. Hwang, Appl. Phys. Lett. 77 (2000) 124.
[15] C. Zhou, D.M. Newns, J. Appl. Phys. 82 (1997) 3081.
[16] C.S. Hwang, J. Appl. Phys. 92 (2002) 432.
[17] B. Chen, H. Yang, L. Zhao, B. Xu, X.G. Qiu, B.R. Zhao, X.Y. Qi, X.F. Duan, Appl. Phys. Lett. 84 (2004) 583.
[18] L. Kim, J. Kim, D. Jung, J. Lee, Thin Solid Films 475 (2005) 97.
[19] Xavier Cartoixà, Lin-Wang Wang, Phys. Rev. Lett. 94 (2005) 236804.
[20] Sanjib Senapati, Amalendu Chandra, J. Phys. Chem. B 105 (2001) 5106.
[21] S.D. Flavio, C.S.L. Rita, T.K. Lauro, Langmuir 21 (2005) 602.
[22] R. Tsu, D. Babic, Appl. Phys. Lett. 64 (1994) 1806.
[23] D.R. Penn, Phys. Rev 128 (1962) 2093.
[24] R. Zallen, The Physics of Amorphous Solids, Wiley-Interscience, New York, 1983, p. 277.
[25] Q. Jiang, H.Y. Tong, D.T. Hsu, K. Okuyama, F.G. Shi, Thin Solid Films 312 (1998) 357.
[26] Q. Jiang, H.X. Shi, M. Zhao, J. Chem. Phys. 111 (1999) 2176.
[27] Q. Jiang, X.Y. Lang, Macromol. Rapid Commun. 25 (2004) 825.
[28] Z. Zhang, J.C. Li, Q. Jiang, J. Phys. D: Appl. Phys. 33 (2000) 2653.
[29] Z. Wen, M. Zhao, Q. Jiang, J. Phys. Chem. B 106 (2002) 4266.
[30] Z. Zhang, M. Zhao, Q. Jiang, Semicond. Sci. Tech. 16 (2001) L33.
[31] R.P. Wang, G. Xu, P. Jin, Phys. Rev. B 69 (2004) 113303.
[32] 〈http://www.webelments.com〉.
[33] 〈http://www.semiconductors.co.uk/〉.
[34] J.D.H. Donnay, H.M. Ondik, Crystal Data Determinative Tables, 3rd ed., US Department of commerce and JCPDS, Washington, DC, 1972 vol. 1. p. A-3.
[35] A.R. Regel, V.M. Glazov, Semiconductors 29 (1995) 405.
[36] R.C. Weast, CRC Handbook of Chemistry and Physics, 69th ed., Chemical Rubber Co., Boca Raton, FL, 1988-1989 ppC-670.
[37] 〈http://fajerpc.magnet.fsu.edu/Education/2010/Lectures/3_Chemical_Bonds.htm〉.